



Texas Water Journal

Volume 13 Number 1 | 2022





Texas Water Journal

Volume 13, Number 1
2022
ISSN 2160-5319

texaswaterjournal.org

THE TEXAS WATER JOURNAL is an online, peer-reviewed journal devoted to the timely consideration of Texas water resources management, research, and policy issues. The journal provides in-depth analysis of Texas water resources management and policies from a multidisciplinary perspective that integrates science, engineering, law, planning, and other disciplines. It also provides updates on key state legislation and policy changes by Texas administrative agencies.

For more information on the Texas Water Journal as well as our policies and submission guidelines, please visit texaswaterjournal.org. As a 501(c)(3) nonprofit organization, the Texas Water Journal needs your support to provide Texas with an open-access, peer-reviewed publication that focuses on Texas water. Please consider [donating](#).

Editor-in-Chief

Todd H. Votteler, Ph.D.
Collaborative Water Resolution LLC

Managing Editor

Chantal Cough-Schulze
Texas Water Resources Institute

Layout Editor

Sarah L. Richardson
Texas Water Resources Institute

Editorial Board

Kathy A. Alexander, Ph.D.
Texas Commission on Environmental Quality

Jude A. Benavides, Ph.D.

The University of Texas, Rio Grande Valley

Gabriel B. Collins, J.D.

Center for Energy Studies
Baker Institute for Public Policy

Ken A. Rainwater, Ph.D.

Texas Tech University

Rosario F. Sanchez, Ph.D.

Texas Water Resources Institute

Michael H. Young, Ph.D.

The University of Texas at Austin



The Texas Water Journal is indexed by [Scopus](#), [Google Scholar](#), and the [Directory of Open Access Journals](#).

The Texas Water Journal is published in cooperation with the Texas Water Resources Institute, part of Texas A&M AgriLife Research, the Texas A&M AgriLife Extension Service, and the College of Agriculture and Life Sciences at Texas A&M University.


Texas Water Resources Institute
make every drop count

Cover photo: A view of the Milky Way over Phoenix Ranch in Jim Wells and Live Oak counties.
©2022 Rey Garza and Jim Quisenberry

Determining Geothermal Resources in Three Texas Counties

Joseph F. Batir^{*1} and Maria C. Richards²

Abstract: The Southern Methodist University Geothermal Laboratory updated their quantification of the geothermal resources within and beneath the Texas oil and gas fields in Crockett, Jackson, and Webb counties as part of the research for the University of Texas Geothermal Entrepreneurship Organization research project DE-EE0008791. Through additional well sites drilled since 2000, the number of bottom-hole temperatures increased from 532 to 5,410. The research improved the methodology to calculate formation temperatures from 3.5 to 10 kilometers (11,480 to 32,800 feet) by using thermal conductivity values more closely related to the county geological formations, incorporating radiogenic heat production of geological formations, and updating the depth to the basement rocks. The results show deep temperatures as hotter than previously calculated, with temperatures of 150 °C (300 °F) possible for Webb, Jackson, and Crockett Counties on average at depths of 3.3, 3.7, and 4.0 kilometers (10,800, 12,100, and 13,100 feet), respectively. A target temperature of 150 °C is considered the minimum for efficient power generation, although cooler temperatures can be useful in other low-temperature applications. Therefore, geothermal resources are a new way to diversify the local electric grid with a baseload renewable energy option. It has the potential of making a significant energy contribution in the future.

Keywords: bottom-hole temperature, electricity, energy, geothermal resource, heat flow, thermal conductivity, 10 kilometers temperatures, radiogenic heat production, Texas, Crockett County, Webb County, Jackson County

¹ Senior Geothermal Geoscientist, Petrotern LLC

² Southern Methodist University Geothermal Laboratory Coordinator, Roy M. Huffington Department of Earth Sciences, Southern Methodist University, Dallas, Texas 75275-0395

* Corresponding author: jbatir@gmail.com

Received 9 January 2021, Accepted 29 April 2022, Published online 25 August 2022.

Citation: Batir JF, Richards MC. 2022. Determining Geothermal Resources in Three Texas Counties. Texas Water Journal. 13(1):27-44. Available from: <https://doi.org/10.21423/twj.v13i1.7130>.

© 2022 Joseph F. Batir and Maria C. Richards. This work is licensed under the Creative Commons Attribution 4.0 International License. To view a copy of this license, visit <https://creativecommons.org/licenses/by/4.0/> or visit the TWJ [website](#).

Terms used in paper

Acronym/Initialism	Descriptive Name
B-CT	Binary-Cycle Technologies
BHT	Bottom-Hole Temperature
COSUNA	Correlation of Stratigraphic Units of North America
DOE	Department of Energy
°C/km	Celsius degree per kilometer
EBK	Empirical Bayesian Kriging
°F/100 ft	Fahrenheit degree per 100 feet
ft	feet
GBES	Geothermal Battery Energy Storage
GHP	Geothermal Heat Pumps
GLO	Texas General Land Office
km	kilometer
kW	kilowatt
MW	megawatt
mW/m ²	milliwatt per meter squared
NGDS	National Geothermal Data System
RHP	Radiogenic Heat Production
RRC	Texas Railroad Commission
SMU	Southern Methodist University
Texas GEO	Texas Geothermal Entrepreneurship Organization
μW/m ³	microwatts per meter cubed
Wm ⁻¹ K ⁻¹	Watts per meter Kelvin

INTRODUCTION

A vast amount of geothermal resources (heat, fluids, related minerals and pressure) exists within the Texas geological formations according to the calculations of John et al. (1998a, 1998b). Blackwell et al. (2006) and Richards and Blackwell (2012) examined the extent of the geothermal heat resource, which was again updated as part of a Southern Methodist University (SMU) Geothermal Lab and University of Texas Geothermal Entrepreneurship Organization (Texas GEO) research project (Batir and Richards 2020). This article focuses on primarily the heat portion of the geothermal resources, and thus uses the nomenclature of “geothermal resource” to signify heat stored within the Earth. We re-examined the amount of stored heat in and below the oil and gas fields in Crockett, Webb, and Jackson counties using updated methods for calculation of the temperatures between 3.5 kilometers (km; 11,500 feet [ft]) and 10 km (32,800 ft). While we examine only these three

counties, they are representative of the other counties within their respective regions: Permian Basin, South Texas, and the Gulf Coastal Plain.

In Texas, the deeper a well is drilled, the hotter the temperatures become because of the heat rising from the Earth’s interior and from the naturally occurring radiogenic heat production (RHP) released by the rock minerals (Negru et al. 2008; Robertson 1988). The thick layers of sediments below much of Texas act as a thermal blanket slowing the release of heat through them (Kresic 2010). In the Hill County, where the granitic rock formations are at or near the surface, the geothermal heat flowing from them is naturally high, but it dissipates into the atmosphere faster than it can be felt by humans and is possible to be collected.

The geothermal resource, measured as subsurface temperatures (Figure 1) and the related amount of heat flowing through the Earth at any one location (heat flow), varies across Texas due to changes in geology (Negru et al. 2008). Texas starts

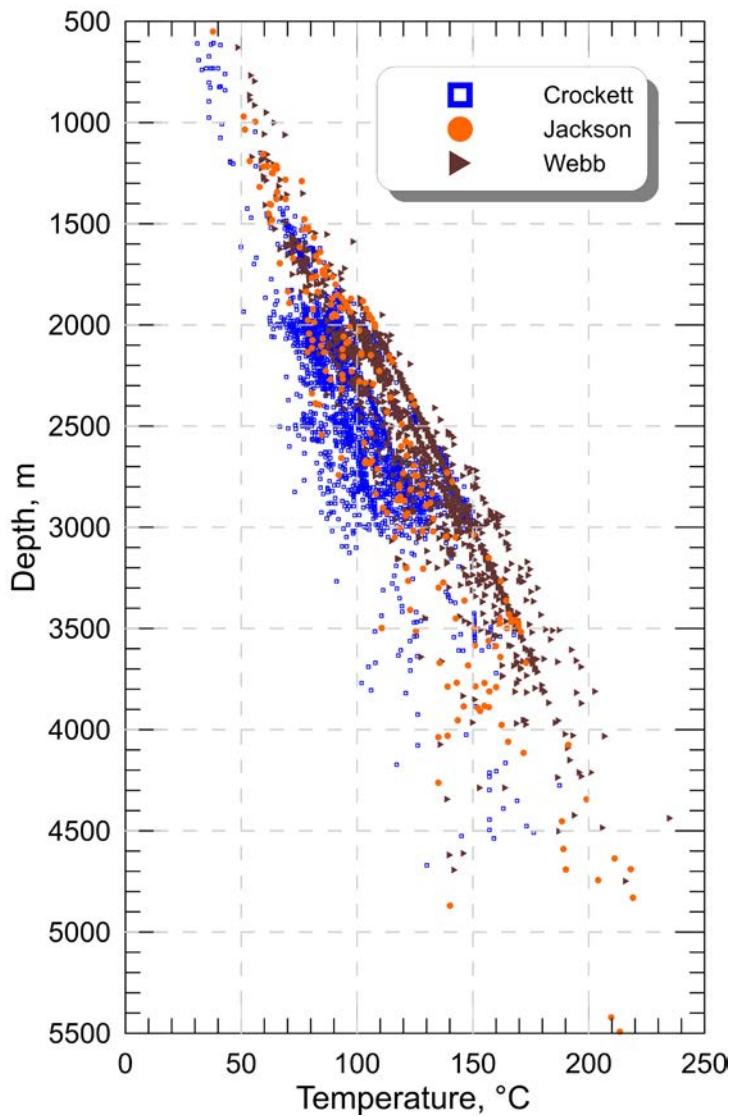


Figure 1. Temperature-depth graph of the corrected bottom-hole temperatures from oil and gas drilled wells for the three counties in this study. Each county represents a region: Crockett – Western Texas; Jackson – Gulf Coast Texas; and Webb – South Texas. Within each county and region, the geothermal resource varies, making detailed assessments necessary.

with high heat flow along the Rio Grande Valley and then quickly changes in the Permian Basin and the Panhandle with temperature gradients among the lowest in the state ([Negaru et al. 2008](#)). North and East Texas contain moderate geothermal resources with development opportunities based on temperature and flow rates in areas such as the Sabine Uplift and the deeper formations such as the Ellenburger (North Texas) and Travis Peak (within the Sabine Uplift; [Richards and Blackwell 2012; Batir et al. 2018](#)). The Gulf Coast and South Texas are known for hot geothermal-geopressedured resources ([John et al. 1998a, 1998b](#); Figure 1). As shown in Figure 1, there are

sites with $\sim 150^{\circ}\text{C}$ (300°F) at 3 km (9800 ft) depth in all three counties, yet most consistently the high temperatures persist in Webb and Jackson counties.

The Texas GEO efforts build on and expand decades of research for geothermal energy in the Gulf Coast related to the geopressed-geothermal studies completed by Texas Bureau of Economic Geology in the 1970s–1990s ([John et al. 1998a, 1998b](#)). Our portion of the project specifically expands on other more recent Texas resource studies ([Richards and Blackwell 2012; Zafar and Cutright 2014; Batir et al. 2018](#)) and the updated temperature-at-depth calculation methodology

([Blackwell et al. 2006](#); [Blackwell et al. 2011a](#); [Stutz et al. 2015](#); [Smith 2016](#); [Smith and Horowitz 2016](#); [Batir et al. 2018](#); [Batir and Richards 2020](#)). This research highlights the importance of detailed geothermal resource mapping to provide the geothermal and oil and gas industries with the expected drilling depths to reach the desired temperature threshold based on the project requirements.

The value in reassessing the geothermal resources base is currently important because of the opportunity to use in Texas the new energy-conversion technologies and methodologies for both direct-use and electrical projects. In addition, extensive amounts of new drilling data from the shale gas revolution provide direct measurements of the Earth's resources. Further outside influences include an increased demand for reliable power that is resilient against weather-related hazards and provides greater grid stability. Companies aiming to increase renewable energy installations and/or carbon reduction can use this research too.

To accomplish this geothermal resource assessment update, we examined in-depth the temperature, formation thermal conductivity, and radiogenic heat within Crockett, Webb, and Jackson counties for each sedimentary formation targeted for oil or gas extraction. The detailed lithologies and bottom-hole temperatures (BHT) from oil and gas well logs provide measured temperatures for 0.6 km to 5 km (1,970 to 16,400 ft) depth. From these values the modeled temperatures from 5 km to 10 km (32,800 ft) below the ground surface were calculated.

BACKGROUND ON GEOTHERMAL RESOURCES

When people hear the word “geothermal,” they may conjure pictures of Yellowstone National Park and volcanoes or geysers; others think of the cooling and heating of homes or buildings with geothermal heat pumps (GHP). Although GHPs or ground source heat pumps are an efficient means of heating and cooling buildings, they are not intended for the generation of electricity. There are advantages to the shallow GHP installations (usually less than 200 meters [-600 ft]) as this resource is available everywhere in Texas. Using the shallow geothermal resource for cooling and heating a home or building is considered a first step in reducing our individual electrical load for the life of the building. Residential heating and cooling account for 40% of the consumer consumption of electricity in Texas ([EIA 2009](#)). Thus, installation of GHPs is one of the more efficient ways to reduce base load requirements for our existing power plants on extremely cold or hot days ([Egg 2021](#)).

In the context of this article, we are focused on the geothermal resource deeper than GHPs and on the production of hot geothermal fluids, or geothermal brines for use in large district energy systems or driving electrical generations. The source

of this energy is from the stored and continuously heated fluids that occur naturally within the deep geologic formations. Many if not all of these formations have been explored and exploited because of their role as oil or gas reservoirs.

The state of Texas stated that deep geothermal resources are to be treated and produced as mineral resources, separate from the oil and gas mineral right in the Texas Geothermal Resources Act of 1975 as part of the Texas Natural Resource Code 141.003 ([Texas Nat. Res. Code 141 § 003](#)). The geothermal resources in Texas includes the heat, fluids (brines), and related byproducts.

Within the fluids are minerals of economic value that vary in type and quantity. For example, in southern California, a large lithium extraction facility is being built to mine the geothermal fluids for lithium using the heat as part of the processing ([Scheyder 2021 July 2](#)). As the Texas deep formation fluids are considered high in total dissolved solids, opportunities exist to mine minerals and then use the fluids as part of a heat extraction process. For example, the city of McAllen, Texas is currently working towards using the geothermal fluids produced from the oil wells in a desalination plant. It would use the heat and fluids from the deep resource in the desalination process, and the resulting clean water would be used to provide additional fresh water for the community and replenish the aquifer ([Flake 2014 Nov 4](#)).

Although there are companies today openly discussing development of geothermal resources in Texas ([Cutright 2013](#); [Malik 2021 April 22](#)), project economics are often stated as a primary reason for limiting the oil and gas industry involvement in geothermal development ([Richter 2018 Sep 12](#)). The geothermal power industry is based on a 20-year business model with high upfront capital expenses paid back with a known income (purchase power agreements) following the utility model. In contrast to the utility model, the oil and gas industry follows the commodity model with the return on investment generally in a few years.

Geothermal Power Development

The commercial interest in deep geothermal resources are heat, pressurized fluids, and mineral content, all varying on a community to regional scale. These resources can be used in numerous ways, including making super chilled water with absorption chilling, direct use of heat in industrial processes, district energy heating for multiple buildings, and generation of electrical power from small-scale (25 kilowatts [kW] to 1 megawatt [MW] power plants) to large-scale (tens to hundreds of MW power plants). Discussions of converting existing oil and gas wells and/or depleted fields into geothermal electrical production (usually considered low temperature; [Boak et al. 2021 Jan](#)) focused on using kW sized power plants. Now there

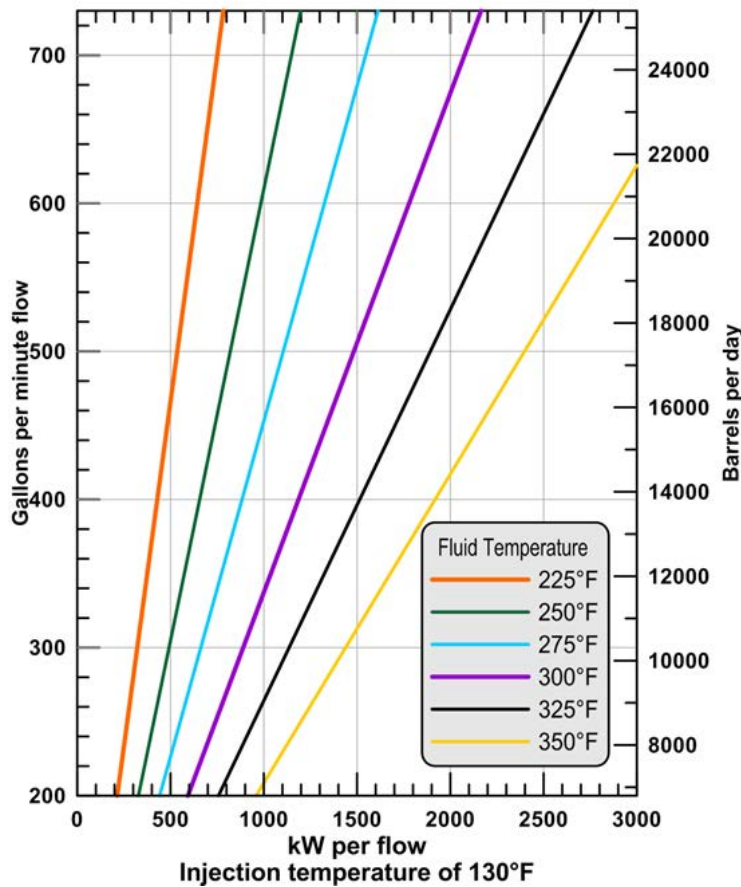


Figure 2. Southern Methodist University Geothermal Laboratory comparison of fluid flow rates and temperatures versus the potential output from a generic geothermal power plant, based on Figure 7.3 in Tester et al. (2006). 1000 kilowatts (kW) is equal to producing 24,000 kilowatt-hours in one day (kWh/day). The 2020 average daily rate for a Texas home is 37.3 kWh/day (EIA 2020). New methods for extracting geothermal resources are being developed that do not use produced fluids and/or include changes in surface technology that this graphic may not represent.

are companies researching how to drill very high temperature ($>200^{\circ}\text{C}$ [392°F]) wells or deepening existing oil and gas wells within the Texas sedimentary basins for MW sized power plants. To learn more about companies involved in geothermal projects, contact organizations such as Texas Geothermal Alliance or the international organization Geothermal Rising.

The geothermal power plant is considered “always on,” as it can produce power 24/7 as a baseload resource. Depending on the size, geothermal power can also assist the grid by being load-following to reduce energy imbalances, and the turbine provides a spinning reserve for unexpected transmission failures. It also offers operational flexibility, which assists with integrating intermittent resources, such as wind and solar, to the grid.

Geothermal electrical projects fill a small footprint, compared to other types of power plants, with kW machines that

are either shipped in containers ready to be used, or MW power plants with machines built onsite. Binary-Cycle Technologies (B-CT) use the low-temperature fluids greater than or equal to 85°C (185°F), e.g., wastewater from oil and gas fields, to generate electricity in the kW range (Moya et al. 2018; Thibedeau 2019 Nov 1). The B-CT generate power based on a secondary fluid that boils at a lower temperature than water, therefore machine efficiency increases with greater temperature differentials between the produced hot fluid (well fluids) and a cooling fluid (air or water). The expected minimum well temperature for consistent power generation during the Texas summers is approximately 125°C (250°F). The currently available power systems require large amounts of hot fluid flow rates – typically in the 1000s of barrels/day (Figure 2). The B-CT cooling side can come from an air inlet system, similar to natural gas plants, or surface water. Projects that use water for the cooling

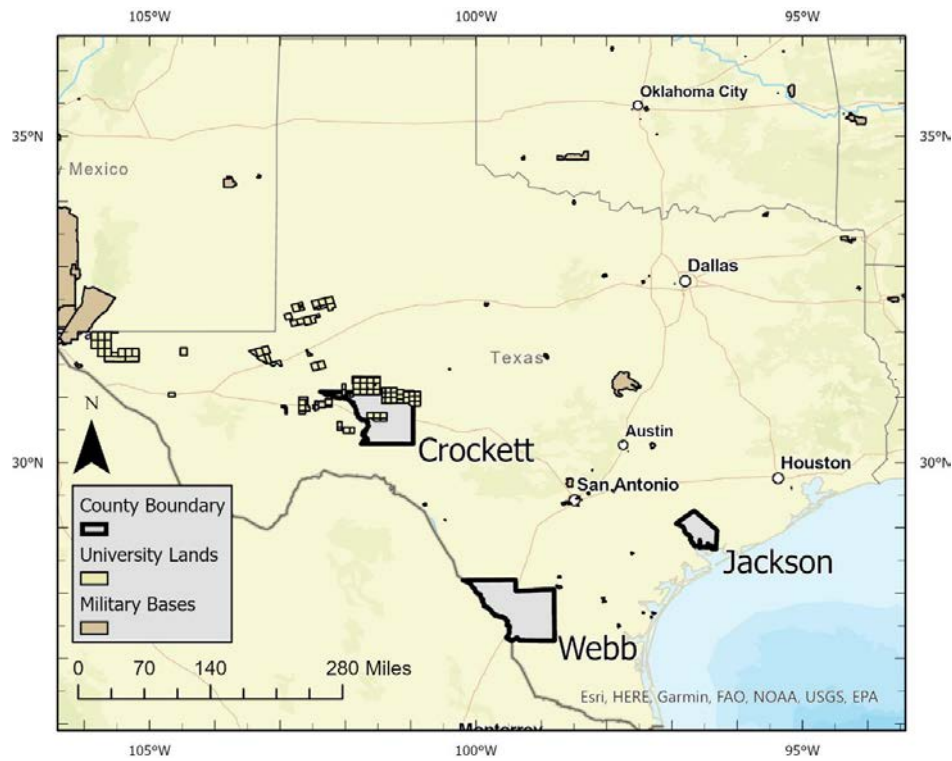


Figure 3. Location of the researched counties shaded in grey along with the potential users of geothermal resources, which are University of Texas land holdings, military bases, and major cities.

cycle may use double the flow rates of the geothermal fluid flow yet have a smaller footprint. There are opportunities for water cooling with treated wastewater, ocean water, or rivers in Texas making the use of a cooling tower a design consideration.

An advantage of using geothermal fluids is the ability to combine them with other technologies to expand and add value to both resources, e.g., solar, wind, batteries, desalination, salt ponds, and other onsite waste heat. Green et al. (2021) modeled the combination of solar plus geothermal energy and existing oil and gas wells for geothermal battery energy storage (GBES) to create a consistent solar energy source regardless of time of day or weather. Using oil field wells, rather than abandoning them at the end of life, extends their value for decades to come. The GBES model combines the oil well with geothermal fluids, solar, and/or wind to build an energy storage system to equalize the production of electricity available for the grid and then be able to use the stored energy for either peak load or as a consistent baseload.

The Texas General Land Office (GLO) had a geothermal lease sale along the Gulf Coast in the last decade, although no geothermal power was developed. Both the Texas Rail-

road Commission (RRC) and GLO established forms and permits for commercializing its use. Unless the fluid is used for desalination or battery storage, the wells for reinjection of the fluids includes permits through the RRC and additional permits through the Texas Commission on Environmental Quality. Geothermal developers will follow a similar permitting and reporting process to the oil and gas industry (OpenEI.org 2016). Therefore, the state of Texas is ready for geothermal development using all aspects of the resource below the surface.

RESEARCH FOCUS

The research area for this research includes Crockett, Webb, and Jackson counties (Figure 3). They were chosen based on four factors: 1) having higher than background heat flow (Blackwell et al. 2011a and 2011b); 2) having oil and gas wells drilled within the last 20 years that are fairly evenly distributed across the county; 3) being geologically representative of the surrounding region; and 4) including possible end-users (e.g., military base, University of Texas Lands ownership, or oil field equipment) if resource evolution led to electricity produced or

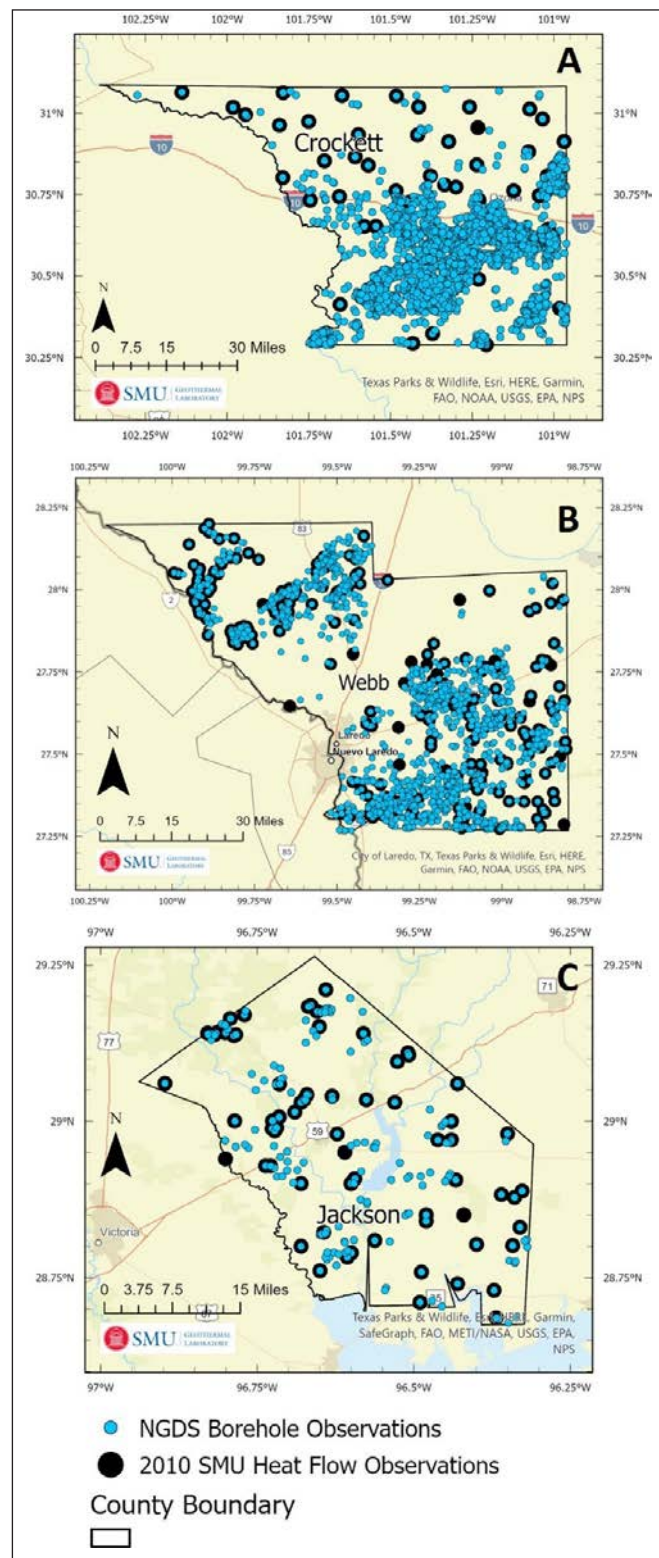


Figure 4. Temperature site data density maps for Crockett, Webb, and Jackson counties. The black circles represent Southern Methodist University heat flow data from Blackwell et al. (2011a, b, c), and the blue circles represent the updated temperatures from the National Geothermal Data System (NGDS 2020) borehole observation file (NGDS 2014), for a combined total of 5,410 well sites.

industry for direct-use applications. The additional oil and gas well data included BHTs in all three counties deeper than 1 km (3,280 ft), and the total number of wells increased from 532 to 5,410 sites. These sites are more evenly distributed both throughout the counties and vertically to depths of 5 km (Figure 1 and Figure 4).

The focus here is on specific counties, whereas the SMU node of the National Geothermal Data System (NGDS 2020) contains temperature and heat flow data for approximately 16,000 wells in Texas, plus other related well information for onshore and offshore sites for over one million wells.

Calculating Deep Temperatures

The temperature calculations assume the study area is at steady state and heat travels by pure conduction through the formations. The method used for this research project differs from using just the temperature gradient to calculate the deep temperatures. We are able to calculate temperatures below known values by incorporating detailed heat flow (thermal conductivity model and temperature gradient) plus the amount of RHP of both the sedimentary section and the basement rocks based on the detailed lithology columns for each county (Batir and Richards 2020).

Temperature-at-depth values start from the surface temperature, BHT, and heat flow value at each well site as inputs into the second derivative of the heat diffusion equation (Blackwell et al. 2006; Stutz et al. 2015; Smith 2016; Smith and Horowitz 2016; Batir et al. 2018; Batir and Richards 2020). Next, the combined heat flow, thermal conductivity model, detailed sedimentary section, and basement properties are used to calculate formation temperatures to depths of 10 km (32,800 ft; Smith 2016; Smith and Horowitz 2016; Batir and Richards 2020). The well-site temperature values are gridded using the Empirical Bayesian Kriging (EBK) interpolation algorithm, which is built to predict values at unmeasured grid cell locations using a spacing of 10 km x 10 km (6 x 6 miles), with the majority of the grid cells having at least one well site. If there are many sites within a grid cell, the values are averaged. Each of the parameters used in the calculation are described in detail in the following subsections. The resulting temperature-at-depth maps are shown in the Results and Discussion section.

Temperature Data

The borehole temperature observation and heat flow datasets from the SMU node of the NGDS (2020) are the source of the temperature data (Figure 4). Both datasets include parameters from oil and gas wells in addition to geothermal wells that are described in the respective NGDS (2014) content model.

Table 1. The amount of change in county averaged parameters compared to the Blackwell et al. (2011a, 2011b, and 2011c) published results in top chart. Bottom chart are the 2020 average values to show general trends in this research project.

County	Temperature % increase	Heat flow % increase	Temperature gradient % increase	Well site thermal conductivity % increase	Well site locations		Rock type percentages SS/SH/LS/SED*
					2011	2020	
Crockett	17	35	30	4	65	3487	5/22/31/42
Jackson	14.6	37	13	20	80	215	30/22/0/48
Webb	13.3	39	14	20	387	1708	21/11/18/50

County	Heat flow mW/m ²	Heat flow standard deviation mW/m ²	Temperature gradient °C/km	Gradient standard deviation °C/km	Depth-weighted site thermal conductivity variation Wm ⁻¹ K ⁻¹	Sedimentary radiogenic heat production μW/m ³
Crockett	77	± 11	32.5	± 4.6	2.11–3.40	0.8
Jackson	81	± 11	34.1	± 4.9	2.27–2.55	1.4
Webb	93	± 9	38.2	± 3.5	2.22–2.49	1.0

* SS: sandstone; SH: shale; LS: limestone; SED: sedimentary rocks in general; mW/m² = milliwatt per meter squared; °C/km = Celsius degree per kilometer; Wm⁻¹K⁻¹ = Watts per meter Kelvin; μW/m³ = microwatts per meter cubed; °C/km divided by 18.2 to calculate °Fahrenheit per 100 feet (°F/100 ft)

Temperature data from wells are impacted by the drilling fluids, in addition to possible recording errors (Richards et al. 2012). Typically, the fluid used for drilling a well is hotter for at least the first 600 meters (1,970 ft) from frictional heating and surface air temperature. At deeper depths, this same fluid is now cooler than the deep-earth temperatures being drilled into, so it cools the formation fluid. The heating and cooling of the wellbore and local formation fluids requires a correction of the well temperature measurements (BHT) taken just after drilling. Wells less than 0.6 km (1,970 ft) were not used because of the irregularities from the impact of drilling. BHT values deeper than 0.6 km were corrected using the SMU-Harrison Correction (Blackwell et al. 2011a; Richards and Blackwell 2012) to change the temperatures gradually from 0 °C (32 °F) at 0.6 km to 19.1 °C (66 °F) below 3.8 km (12,500 ft). This correction increased the average BHT value by 17% for Crockett County, 14.6% for Jackson County, and 13.3 % for Webb County, highlighting a greater number of deep wells in all three counties than previously used (Blackwell et al. 2011a; Table 1).

The additional well data impacted each county. Jackson County contained the fewest well sites in this project with 215, yet the wells are spaced fairly evenly across the entire county (Figure 4). In Webb County, data coverage follows the general trends of the previous 387 wells increasing to 1708 sites for this project, with the increase in well numbers because of expanded oil and gas plays. The Crockett County dataset increased the most, with total numbers of well sites changing from 65 to 3,487 for this project. The additional data impact the southern portion of the county more than the northern half. The new data include many wells drilled since 2005 that generally

include hotter BHTs than the older wells (pre-2000; Figure 1, following the right [hotter] temperature-depth trend). The reason for these hotter wells is currently not investigated but is hypothesized to relate to the more recent drilling technology and more rapid well completion. The wells may be equilibrating faster than the older wells, causing the BHT to be hotter (closer to original in-situ value) in the deep wells.

Thermal Gradient

In order to calculate a well gradient value (Celsius per kilometer [°C/km]) the average ground surface temperature (Gass 1982) is the top temperature for each corrected BHT. Gradient values are generally similar to each other within a local area unless there are faults or lithology changes (Blackwell 1971). Therefore, the gradients were reviewed to find outlier values (beyond two standard deviations of a data cluster (10 x 10 km [6 x 6 miles])), removing a total of 416 well gradients to remove potential erroneous data.

Thermal Conductivity Determination

The parameter of thermal conductivity varies based on the rock minerals, formation age, pressure, pore space, and fluid chemistry (Robertson 1988). In Texas there are limited measured thermal conductivity values for the sediments below 1 km and none in the three studied counties. McKenna and Sharp (1998a) measured thermal conductivity of the Wilcox and Frio formations at three localities in the South Texas portion of the Gulf Coast Basin. Their results show how thermal

conductivities of Wilcox and Frio sandstones range from 2.06 to 5.03 watts per meter Kelvin ($\text{Wm}^{-1}\text{K}^{-1}$) based on changes in the porosity, which ranges from 2.4% to 29.6%, with lower porosity trending with higher thermal conductivity. Although formations are named after their rock type, e.g., Eagle Ford Shale, Wilcox Sandstone, these include mixed layers of sandstone, shale, and silts. McKenna and Sharp (1998a) highlight the importance of location-specific measurements for site-specific analysis.

This project incorporates the thermal conductivity values used in the past with additional refinement. We started with the Blackwell et al. (2011a) use of the Anadarko Basin formation values from core and cuttings measured on the divided bar (Gallardo and Blackwell 1999; Carter et al. 1998). These values were used primarily for Crockett County along with updates for evaporites by Frone et al. (2015). For more details, see Appendix A in Final Report, Batir and Richards (2020). For East Texas, we incorporated the methods used in the deep direct-use report (Batir et al. 2018; Turchi et al. 2020), which used thermal conductivity values based on the values of Pittman and Rowan (2012). They assigned thermal conductivity values for each formation based on the mineralogy, specifically percent sandstone, shale, silt, and limestone for Louisiana formations that extend into Texas. These values were assigned an estimate of ~10% error based on the typical range of values for multiple samples from the same formation run on the divided bar at SMU Geothermal Laboratory.

The thermal conductivity values are then assigned to formation depths based on detailed stratigraphic columns from the sections of the Correlation of Stratigraphic Units of North America (COSUNA) data compilation (AAPG 1994), in addition to publications with county-level stratigraphy details (Baker 1995; Galloway 2008; Hackley 2012; Hamlin 2009; Kincade 2018; Lambert 2004; McDonnell et al. 2008) and use of formation Tops data from WellDatabase (2020). Using this level of detail allows the incorporation of the full geological column for each well and every formation is given a thickness weighted thermal conductivity value for the specific well.

Heat Flow Calculations

Heat flow measurements are assumed to be one dimensional with heat traveling upward out of the surface of the Earth, in a purely conductive thermal regime, and constant over the measurement distance. The weighted thermal conductivity values are used to calculate heat flow for each well by multiplying gradient times thermal conductivity (Blackwell et al. 2011a; Horowitz et al. 2015; Smith 2016; Smith and Horowitz 2016; Batir and Richards 2020).

Previous work in these counties by the SMU Geothermal Laboratory included heat flow sites (Blackwell and Richards 2004; Blackwell et al. 2011a) and other data used by Bureau of

Economic Geology at the University of Texas at Austin (Zafar and Cutright 2014).

Radiogenic Heat Production Model

RHP is produced by the decay of naturally occurring radioactive minerals within rocks and varies based on rock type (e.g., limestones are low, and shales are high RHP) and age (younger rocks contain more RHP [Hasterok and Webb 2017]). This is one of the primary sources of the heat stored within the deep formations within the Texas basins; the other is from the Earth's core and mantle releasing heat. McKenna and Sharp (1998b) measured RHP values for limestone, mudstone, and sandstone in Webb County that we incorporated into our model. Once the lithologic sections were completed for the thermal conductivity models, the RHP (0.8–1.4 microwatts per meter cubed [$\mu\text{W}/\text{m}^3$]) was added to allow a site-by-site lithology and thickness-weighted value rather than a constant $1 \mu\text{W}/\text{m}^3$ as used in previous SMU studies (Blackwell et al. 2006; Blackwell et al. 2011a). Along with the expansion of the amount of heat production, this project also updated the depth to the basement rock mapped from seismic reflection cross-sections and seismic velocity data (Agrawal et al. 2015; Čermák et al. 1991). Previous studies allowed for a maximum of 13 km of sediments at the surface. This project increases sedimentary depth up to 15 km in Webb County and 20 km in Jackson County because of the Gulf Coast sediments being both younger and more unconsolidated than other U.S. basins previously studied (Gallardo and Blackwell 1999). These increased sedimentary thickness estimates agree with recent drilling activity and the estimated depth to basement contours (Blackwell et al. 2006).

Input Data Error Values

For this research project, the updates include 10 times more well sites, a consistent method for correcting the BHT, revised thermal conductivity values, and updated methods for calculating heat flow and temperature-at-depth. The input parameter errors are primarily related to the oil and gas recorded well log header BHT, the thermal conductivity assignments, and the resolution of the county based stratigraphic sections.

Most large errors in temperature and depth were initially removed while cleaning the data. Next data errors were removed by comparing the site gradients using two standard deviations from other nearby wells. This entailed using ESRI ArcGIS software to highlight wells within a $10 \times 10 \text{ km}$ ($6 \times 6 \text{ miles}$) surface area and $\pm 1 \text{ km}$ (3,280 ft) of depth for each well. If the well temperature value is higher or lower than the neighboring wells by two standard deviations, the reviewed well site is removed from the data set. The resulting temperature error is still considered up to $\pm 10\%$ because of many unknowns.

The assigned thermal conductivity values were given an error of up to $\pm 10\%$ because of the lack of local formation measurements. There is an additional $\pm 5\%$ error for the thermal conductivity associated with errors in the recorded depth of the BHT measurement, i.e., conductivity assigned to wrong formation. This is a cumulative error to capture the drilling rig height above ground level and temperature logging gear precision. The SMU Geothermal Lab also added error as part of the methodology used to scale the thickness of the formations at each well site as part of the assignment of the thermal conductivity value.

The temperature, gradient, and thermal conductivity errors all combine to a potential site heat flow error of $\pm 25\%$, similar to other related work ([Richards et al. 2012](#)).

RESULTS AND DISCUSSION

Using the measured values of temperature at a specific depth, determined thermal conductivity, stratigraphy, calculated heat flow, and assigned in situ RHP, we calculated temperature values for the studied Texas counties to 10 km (32,800 ft) depths and used these results to produce temperature-at-depth maps for geospatial interpretation.

The process of calculating these temperatures includes models, which use the site-specific temperature and depth to accurately depict the temperatures to that depth, and then incorporates surrounding well information and other parameters (lithology, RHP) to calculate temperatures for intermediate depths and depths to 10 km (32,800 ft). The deepest BHT is 259 °C (498 °F) at 6.3 km (20,700 ft) depth in Webb County; in Jackson County the BHT is 214 °C (417 °F) at 5.5 km (18,000 ft) depth; and in Crockett County the deepest BHTs are on average 160 °C (320 °F) at 4.5 km (14,800 ft) depth (Figure 1). There is no direct temperature measurement, thermal conductivity, or RHP beyond these deepest BHT values. Although there are many well sites between 3.5 km (11,500 ft) and the deepest site in each county, in general, the majority of the well data are less than 3.5 km, and therefore the temperature maps deeper than 3.5 km include an additional uncertainty in the values calculated for resource estimation.

The new county heat flow and temperature maps are more detailed in their geological understanding than previous maps (see the maps in the next section). Terrestrial heat flow values increased by 35%, 37%, and 39% for Crockett, Jackson, and Webb counties, respectively, in comparison to past results by Blackwell et al. ([2011a](#) and [2011b](#)) and Blackwell and Richards ([2004](#); Table 1). The increases in heat flow are reflective of the heat flow parameters: geothermal gradient and thermal conductivity. The average county-wide geothermal gradient (surface to BHT) increased by 30%, 13%, and 14% for Crockett, Jackson, and Webb counties, respectively, because of the higher resolution from additional well BHT data. Crockett County's

30% increase is related to a large dataset of BHT data from well log headers more recent than 2005. These include values hotter than the well logs from pre-2000. As the BHT values are reflective of drilling, a future study of the new drilling techniques and related impact on BHT is suggested to determine the necessary amount and type of BHT correction. Therefore, the highest temperatures used in this study for Crockett County may be even higher than actual in situ temperatures.

We used the thermal conductivity values that Pitman and Rowan ([2012](#)) assigned to individual formations in Louisiana for their related formation in Texas. This change from Blackwell and Richards' ([2004](#)) thermal conductivity model to the Pitman and Rowan ([2012](#)) values increased the overall thermal conductivity by approximately 20% for wells in Jackson and Webb counties. Although the values for Jackson and Webb counties increased significantly, these thermal conductivity values are more geologically correlated than the previous general model of Blackwell and Richards ([2004](#)) and Blackwell et al. ([2011a](#)). In Crockett County, the thermal conductivity values increased by only 4% because we used the same Anadarko Basin values ([Gallardo and Blackwell 1999](#); [Carter et al. 1998](#)) as the previous mapping ([Blackwell and Richards 2004](#); [Blackwell et al. 2011a](#) and [2011b](#)). This project increased the detail of the formations to account for improved calculations and correlation methods for depth to formation and formation thickness.

The additional well data density shows significant heat flow heterogeneity, which is considered a real geological variation as opposed to increased data error. The cleaning of the data using data clusters of 10 x 10 km (6 x 6 miles) may have removed resource anomalies, but at this assessment level, elimination of outliers caused by drilling or human entry error was the goal. Additionally, all the heat flow values were calculated using the same numerical model, regardless of previous heat flow determinations. Thus, the heterogeneity is considered the result of variation within the input data (corrected BHT and thermal conductivity) instead of variations in the heat flow calculation methodology.

Temperature Maps 3 km to 10 km

Temperature was calculated from surface to 10 km (32,800 ft). Temperature-at-depth maps are presented for depth slices 3.5 km (11,500 ft), 5.0 km (16,400 ft), and 10 km (32,800 ft). The 3.5 km depth slice contains the most direct measurement correlation (see Figures 1 and 4 for the temperature-depth scatter plot and well locations within each county, respectively). The 5.0 km depth slice is the limit of temperature measurement, and the 10 km depth slice is calculated temperature models based on the input data. The deepest temperature measurement is 6.3 km (20,700 ft) deep, and as such there are no direct temperature measurements below 6.3 km. The 10 km

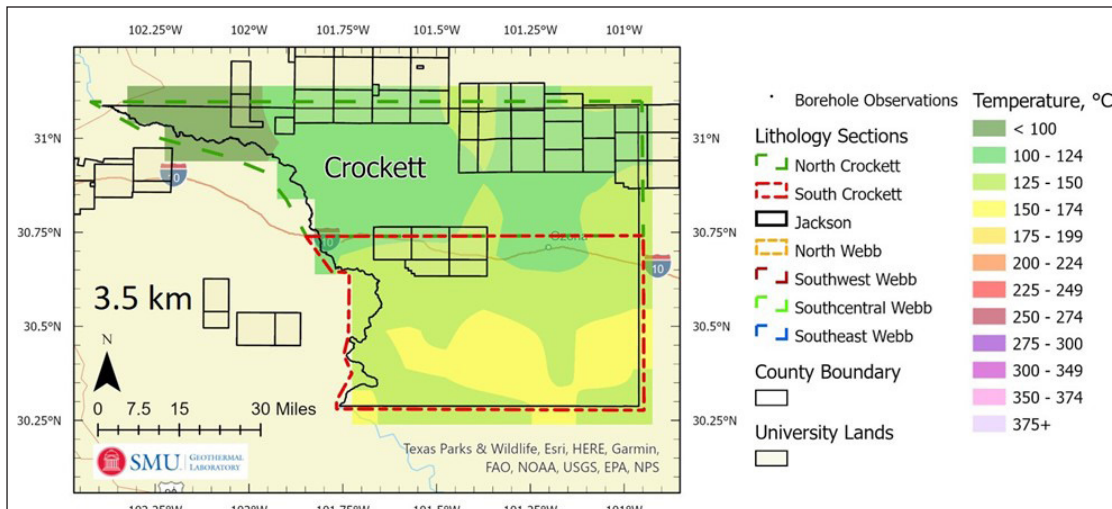


Figure 5. Crockett County temperature at 3.5 kilometers (km; 11,500 feet) depth. The temperature shows a general increase from north and west to south and east. The University Lands are highlighted as boxes on the maps. The dashed lines represent the North and South lithology cross-section areas ([Batir and Richards 2020](#)).

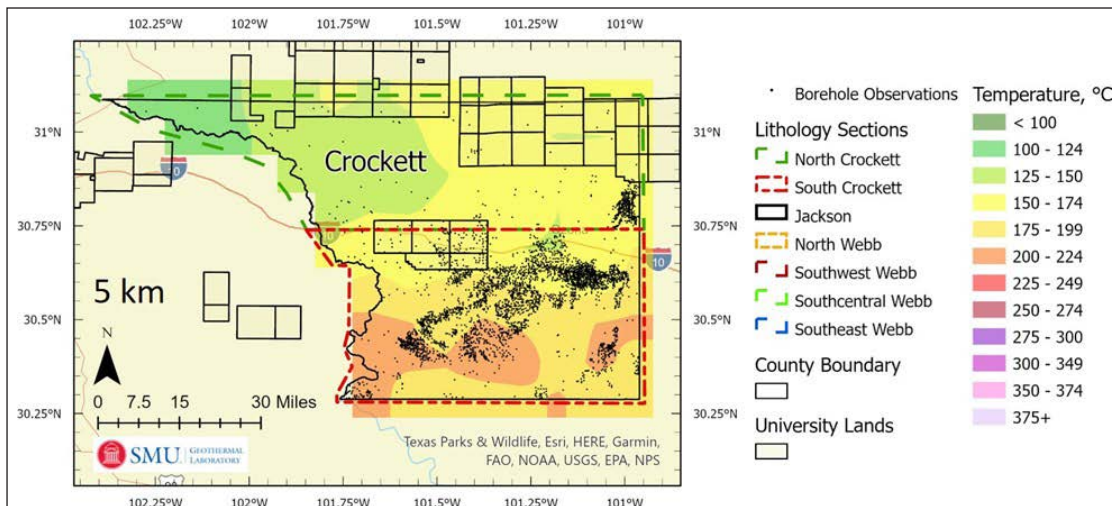


Figure 6. Crockett County temperature at 5.0 kilometers (km; 16,400 feet) depth. A similar trend of warmer temperatures going from the northwest to south and east is visible. Surface well locations are displayed as small black dots for reference but are not this deep (Figure 1). The majority of Crockett County is over 150 °C (300 °F) at this depth.

depth slice is presented as a future depth goal for geothermal energy production with increased technology development and innovation. Companies drilling geothermal wells require specific temperatures for their project and use the estimated temperatures at 10 km (32,800 ft) as a framework for their depth-to-drill calculations. Temperature maps at 5 km and beyond have an uncertainty of $\pm 25\%$, equivalent to the estimated error associated with BHT derived heat flow ([Richards et al. 2012](#)). Deeper equilibrium temperature logs and local thermal conductivity measurements are necessary to reduce the uncertainty in the deeper modeled temperature values.

Crockett County

Crockett County temperature-at-depth maps are presented for the 3.5 km (11,500 ft), 5.0 km (16,400 ft), and 10 km (32,800 ft) depth slices (Figures 5, 6, and 7, respectively). The highest temperatures at the respective depths are in the southern and eastern portions of the county. Temperatures are not above 150 °C (300 °F) within the University Lands boundaries (square grids) until 5 km depth, although there are areas at 125–150 °C at 3.5 km depth, which may be prospective for geothermal electricity generation using new low-temperature technologies. The southern region of the county, as part of the

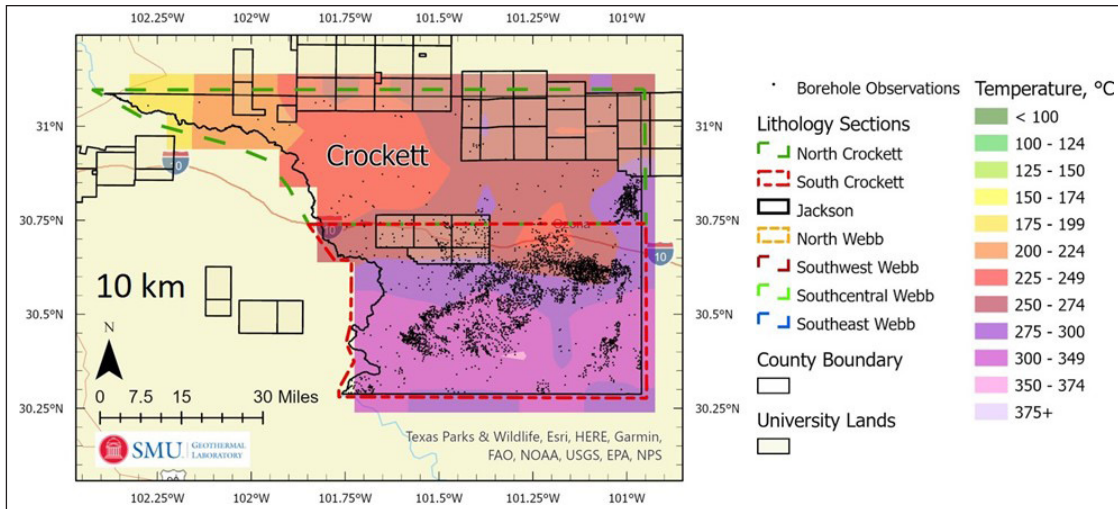


Figure 7. Crockett County temperature at 10 kilometers (km; 32,800 feet), with surface well locations displayed as small black dots. While data sites are displayed on this map, there are no direct temperature measurements at this depth. The modeled temperatures reach greater than 300 °C in the south.

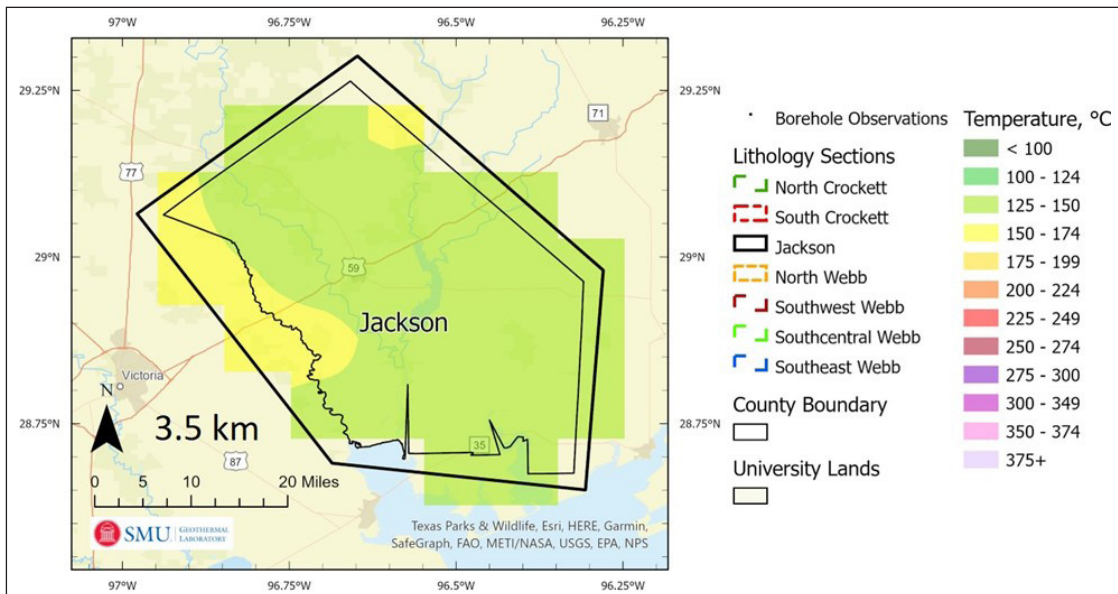


Figure 8. Temperature at 3.5 kilometers (km; 11,500 feet) depth in Jackson County. Higher temperatures are mapped along the western boundary and near the northern corner of the county. One county lithology cross-section was used.

Val Verde Basin, may be prospective for geothermal electricity production, which could be immediately used in ongoing oil and gas exploration and production.

Jackson County

Jackson County temperatures at 3.5 km (11,500 ft), 5.0 km (16,400 ft), and 10 km (32,800 ft) are presented in Figures 8, 9, and 10, respectively. Modeled temperatures are warmer along

the western and northern boundary of the county and generally lower to the east. This trend becomes more pronounced with increasing depth, although temperatures at 10 km are modeled temperatures and therefore include more uncertainty. The higher temperatures along the western mapped boundary suggests there is geothermal electricity potential that could be generated for the grid or used for industrial purposes in the county.

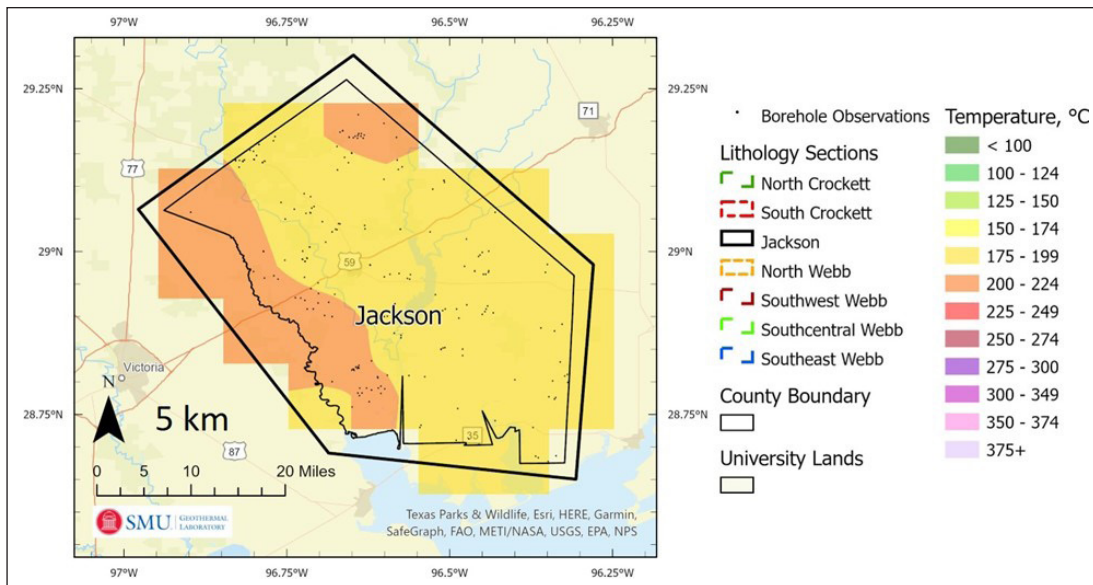


Figure 9. Temperature at 5.0 kilometers (km; 16,400 feet) depth in Jackson County, with data locations shown as small black dots, although most wells are this deep (Figure 1). This is the deepest temperature map with near direct temperature measurements to support the temperature gridding. At this depth, the whole county is above 150 °C (300 °F).

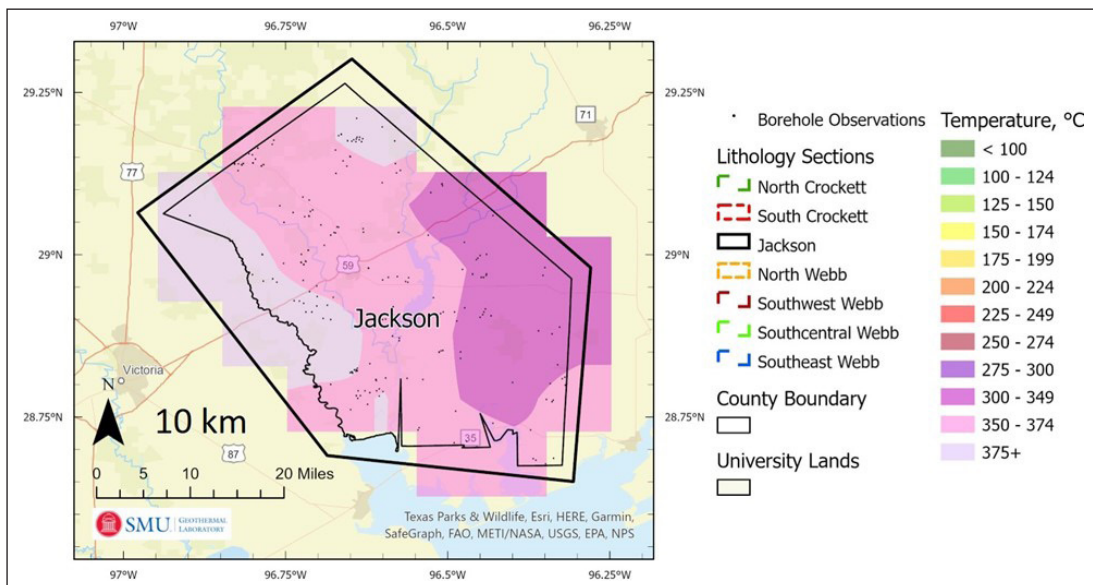


Figure 10. Modeled temperature at 10 kilometers (km; 32,800 feet) depth in Jackson County. While the entire county contains high temperatures, there are no direct temperature measurements at this depth and uncertainty is $\pm 25\%$, which could be as high as ± 100 °C (212 °F). The temperatures for 10 km range from 300 to 375+ °C (572 – 700 °F).

Webb County

Temperature at depths of 3.5 km (11,500 ft), 5.0 km (16,400 ft), and 10 km (32,800 ft) are presented for Webb County in Figures 11, 12, and 13, respectively. Webb County shows a general trend of warmer temperatures moving from the northwest to the southeast. The city of Laredo has estimated temperatures at 150–174 °C (300–345 °F) at 3.5 km

(11,500 ft), which is prospective for geothermal electricity production using the newer geothermal systems being developed today, e.g., Sage Geosystems. There are large numbers of data in the 3 to 4 km (9,800 to 13,100 ft) depth range that support these temperature estimates (see Figure 1). These temperature trends are modeled to continue in a similar pattern to 10 km depth, although there is only one data point deeper than 5 km (16,400 ft), which is 258 °C (496 °F) at 6.28 km (20,600 ft).

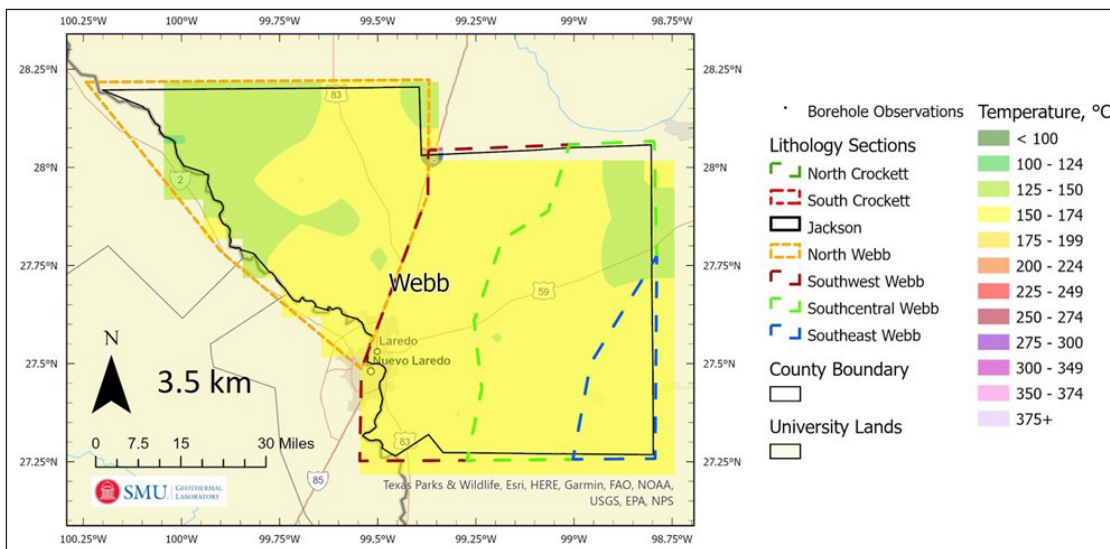


Figure 11. Temperature at 3.5 kilometers (km; 11,500 feet) depth in Webb County. The majority of the county is within the 150–174 °C (300–345 °F) temperature range. The only areas outside this temperature range are the northwestern and eastern corners of the county. Dashed lines represent each area of the four lithology cross-sections (Batir and Richards 2020).

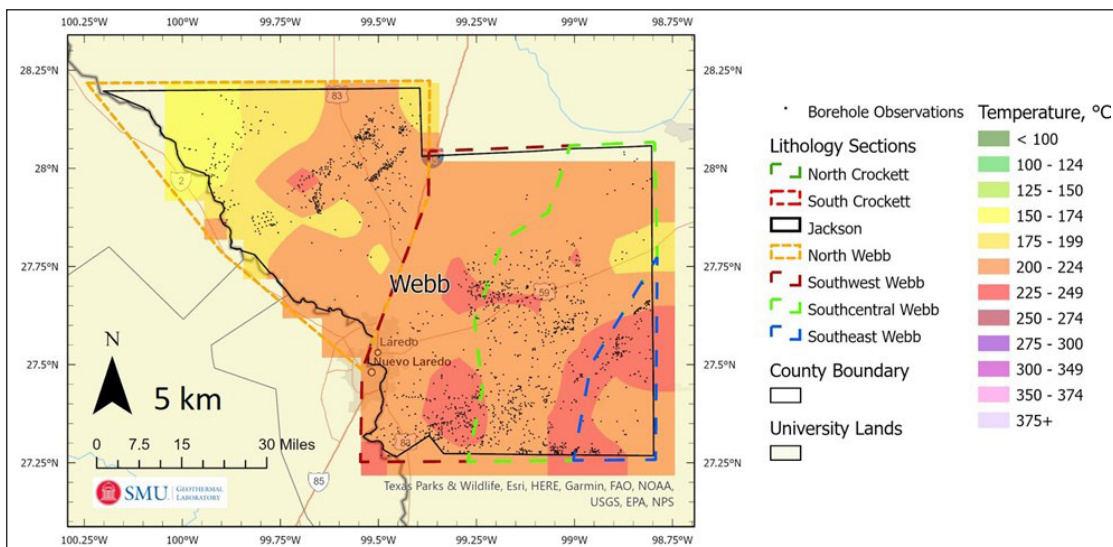


Figure 12. Temperature at 5.0 kilometers (km; 16,400 feet) depth in Webb County. Data point locations displayed as black dots. While all the data locations are shown, only two sites are below 5 km and both are above 200 °C (392°F).

NEXT STEPS

The United States is considered a geothermal industry leader for project development in hard rock (volcanic and metamorphic) conditions, as the largest geothermal power producer in the world (NS Energy 2020). The ability to extract the heat from sedimentary formations, such as the Texas oil and gas fields, was first accomplished in Brazoria County (John et al. 1998a, 1998b) as part of the geopressured-geothermal demonstration project, known as the Pleasant Bayou Project. More recently, there were short-term B-CT demonstrations in

Mississippi, North Dakota, and Wyoming for the equipment rather than the basins. To achieve the level of an oil and gas play fairway evaluation, additional geological parameters not covered in this paper need to be reviewed, e.g., fluid flow and chemistry within reservoirs, detailed fault mapping, and pressure regimes. The sharing of knowledge from the oil and gas industry on the nuances of the productive sedimentary formations, i.e., changes in the minerals, porosity, pressure, and so on, will be useful for those exploring and planning geothermal projects in sedimentary basins.

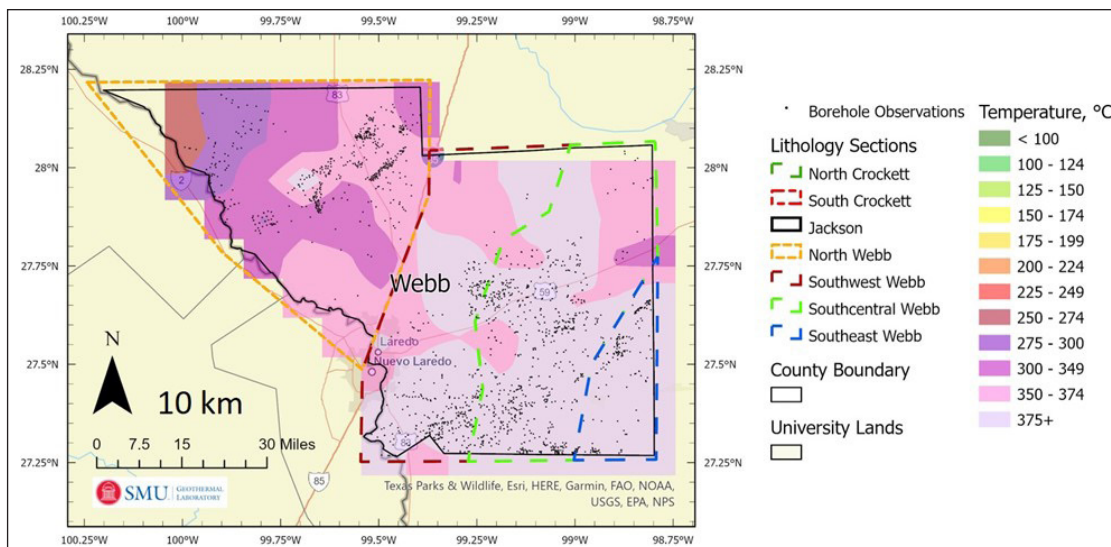


Figure 13. Modeled temperature at 10 kilometers (km; 32,800 feet) in Webb County. Surface well locations are displayed as black dots. At this depth, the temperature uncertainty is $\pm 25\%$, which could be as high as ± 100 °C (212 °F). The highest modeled temperatures (greater than 375 °C [700 °F]) continue to be in the southeastern portion of the county, which suggests there may be additional geothermal resources continuing to the south and east of Webb County.

CONCLUSIONS

Work performed on this project calculated new heat flow values for 5,824 points (5,410 surface locations) in Crockett, Jackson, and Webb counties. This effort for heat flow is an increase of 10 times the previously used data (532 points) for these three counties. In addition, we built detailed lithology sections from the county geology and new thermal conductivity models based on related published models, core measurements, and mineral-matrix derived thermal conductivity values. These combine to expand the density and heterogeneity of the county temperature-at-depth maps from the surface downwards.

The new results show heat flow is higher than previously published, generally by 30–40% with the trends of data being consistently higher for all three counties. This result is reflective of the large dataset containing a 13–30% higher geothermal gradient and a 4–20% increase in thermal conductivity assignments. A $\pm 10\%$ error is assigned to both the gradient and thermal conductivity value, even after removal of well sites considered beyond two standard deviations. The heat flow error of $\pm 25\%$ includes the temperature and thermal conductivity errors.

The county level temperature-at-depth maps are shown for 3.5 km (11,500 ft), 5.0 km (16,400 ft), and 10 km (32,800 ft). Temperature-at-depth modeling incorporated the detailed lithology models along with improved inclusion of sedimentary RHP from measured values and updated basement RHP models to account for the thick sedimentary package of the Texas Gulf Coast. Temperatures are on average 25–50 °C (77 –

122 °F) warmer at 3.5 km (11,500 ft), on the order of a 50% increase in temperature from previous results. Well sites greater than 3.0 km (9,800 ft) depth are plentiful, e.g., 139 in Crockett County, 72 in Jackson County, and 786 in Webb County, with the deepest well at 6.28 km (20,600 ft) in Webb County. The 3.5 km (11,500 ft) temperature-at-depth calculation is directly supported by measured BHT. Beyond this depth, the temperature maps are limited in direct measured values. Temperature maps presented for 10 km (32,800 ft) are based on current geological knowledge but not definitive of actual values since they are calculated and not measured. These deeper temperature maps are to be used as a tool for future research and not used for site-specific evaluations. There are measured temperatures of 150 °C (300 °F) in all three counties between 3.0 and 3.5 km (9,800 and 11,500 ft) depth, therefore already reaching the level of potential use for geothermal electrical production. The next step is to examine formations in these areas for reservoir production potential.

Basic research, such as core thermal conductivity measurements and collection of the well header BHTs in Texas wells, are two items that can improve future geothermal resource understanding. The temperature-at-depth model also includes calculations focused on a new basement RHP model. This is a key development for future heat flow and temperature-at-depth calculations, as it is necessary to understand the basement RHP distribution for accurate temperature modeling when drilling into the basement, beyond the sedimentary package. Each year new research techniques and data acquisition in geophysical

fields improve our understanding of the sediments along the Gulf Coastal Plain and thereby increase our ability to map temperatures and expand formation details. With further study and collaboration, this will result in successful development of geothermal resources in Texas.

REFERENCES

- [AAPG] American Association of Petroleum Geologists. 1994. CSDE, COSUNA, and Geothermal Survey. Tulsa (Oklahoma): American Association of Petroleum Geologists. Data CD-ROM.
- Agrawal M, Pulliam J, Sen MK, Gurrola H. 2015. Lithospheric structure of the Texas-Gulf of Mexico passive margin from surface wave dispersion and migrated Ps receiver functions. *Geochemistry, Geophysics, Geosystems*. 16(7)2221-2239. Available from: <https://doi.org/10.1002/2015GC005803>.
- Baker ET. 1995. Stratigraphic nomenclature and geologic sections of the Gulf Coastal Plain of Texas. Austin (Texas): U.S. Geological Survey. 34 p. Open File Report 94-461. Available from: <https://pubs.usgs.gov/of/1994/0461/report.pdf>.
- Batir JF, Richards MC. 2020. Analysis of geothermal resources in three Texas counties. Dallas (Texas): Southern Methodist University. 60 p. Available from: <https://gdr.openei.org/submissions/1291>.
- Batir JF, Richards MC, Schumann H. 2018. Reservoir analysis for deep direct-use feasibility study in East Texas. GRC Transactions. 42. Available from: <https://publications.mygeogenergynow.org/grc/1034077.pdf>.
- Blackwell DD. 1971. The thermal structure of the continental crust. In: Heacock JG, editor. *The Structure and Physical Properties of the Earth's Crust, Volume 14*. Washington (District of Columbia): American Geophysical Union. Available from: <https://doi.org/10.1029/GM014p0169>.
- Blackwell DD, Richards MC., editors. 2004. Geothermal Map of North America. Tulsa (Oklahoma): American Association of Petroleum Geologists. Scale 1:6,500,000. Available from: <https://www.smu.edu/Dedman/Academics/Departments/Earth-Sciences/Research/GeothermalLab/DataMaps/GeothermalMapofNorthAmerica>.
- Blackwell DD, Negaru PT, Richards MC. 2006. Assessment of the enhanced geothermal system resource base of the United States. *Natural Resources Research*. 15(4):283-308. Available from: <https://doi.org/10.1007/s11053-007-9028-7>.
- Blackwell DD, Richards MC, Frone ZS, Batir JF, Ruzo AA, Dingwall RK, Williams MA. 2011a. Temperature-at-depth maps for the conterminous U.S. and geothermal resource estimates. GRC Transactions. 35. Available from: <https://publications.mygeogenergynow.org/grc/1029452.pdf>.
- Blackwell DD, Richards MC, Frone ZS, Batir JF, Williams MA, Ruzo AA, Dingwall RK. 2011b. SMU Geothermal Laboratory heat flow map of the conterminous United States. Available from: https://www.smu.edu/-/media/Site/Dedman/Academics/Programs/Geothermal-Lab/Graphics/SMUHeatFlowMap2011_CopyrightVA0001377160.jpg?la=en.
- Blackwell DD, Richards MC, Frone ZS, Batir JF, Ruzo AA, Dingwall RK, Williams MA. 2011c. Temperature-at-depth maps for the conterminous U.S., SMU Geothermal Laboratory Maps produced for Google.org. Southern Methodist University Department of Earth Sciences Dallas Texas. Available from: <https://www.smu.edu/Dedman/Academics/Departments/Earth-Sciences/Research/GeothermalLab/DataMaps/TemperatureMaps>.
- Boak J, Cohen AJ, Faroughi S, Soroush H, Richards MC. 2021 Jan. Geothermal Energy – A sustainable alternative to well abandonment. Recorder. Available from: <https://www.csegrecorder.com/articles/view/geothermal-energy-a-sustainable-alternative-to-well-abandonment>.
- Carter LS, Kelley SA, Blackwell DD, Naeser ND. 1998. Heat flow and thermal history of the Anadarko Basin, Oklahoma. *AAPG Bulletin*. 82(2):291-316. Available from: <https://archives.datapages.com/data/bulletns/1998/02feb/0291/0291.htm>.
- Čermák V, Bodri L, Rybach L. 1991. Radioactive heat production in the continental crust and its depth dependence. In: Čermák V, Rybach L, editors. *Terrestrial heat flow and the lithosphere structure* p. 23-69. Germany: Springer Berlin, Heidelberg. Available from: https://doi.org/10.1007/978-3-642-75582-8_2.
- Cutright BL. 2013. Finding geothermal resources for project development. Presented at: Southern Methodist University Geothermal Laboratory Power Plays Conference. Dallas (Texas). Available from: <https://www.osti.gov/servlets/purl/1137016>.
- Egg J. 2021. Geothermal heat pumps are the answer to eliminating electric grid spikes (like we saw in Texas). Geothermal Rising. Available from: <https://geothermal.org/our-impact/stories/geothermal-heat-pumps-are-answer-eliminating-electric-grid-spikes-we-saw-texas>.
- [EIA] U.S. Energy Information Administration. 2009. Household energy use in Texas. Washington (District of Columbia): U.S. Energy Information Administration. Available from: https://www.eia.gov/consumption/residential/reports/2009/state_briefs/pdf/tx.pdf.
- [EIA] U.S. Energy Information Administration. 2020. 2020 Average Monthly Bill- Residential. Washington (District of Columbia): U.S. Energy Information Administration. Available from: https://www.eia.gov/electricity/sales_revenue_price/pdf/table5_a.pdf.

- Flake C. 2014 Nov 4. McAllen eyes geothermal wells for water source. Texas Tribune. Available from: <https://www.texas-tribune.org/2014/11/04/mcallen-eyes-geothermal-wells-water-source/>.
- Frone ZS, Blackwell DD, Richards MC, Hornbach MJ. 2015. Heat flow and thermal modeling of the Appalachian Basin, West Virginia. *Geosphere*. 11(5):1279-1290. Available from: <https://doi.org/10.1130/GES01155.1>.
- Gallardo J, Blackwell DD. 1999. Thermal structure of the Anadarko Basin. *AAPG Bulletin*. 83(2):333-361 Available from: <https://archives.datapages.com/data/bulletns/1999/02feb/0333/0333.htm?msclkid=be3dfbc-c0f111ec9a674a81d07caf41>.
- Galloway WE. 2008. Depositional evolution of the Gulf of Mexico sedimentary basin. In: Miall AD, editor. *Sedimentary basins of the world*. Amsterdam (The Netherlands): Elsevier. 5:505-549. Available from: [https://doi.org/10.1016/S1874-5997\(08\)00015-4](https://doi.org/10.1016/S1874-5997(08)00015-4).
- Gass TE. 1982. The geothermal heat pump. *Geothermal Resources Council Bulletin*. 11(11):3-8. Available from: <https://www.geothermal-library.org/index.php?mode=pubs&action=view&record=7000177>.
- Green S, McLennan J, Panja P, Kitz K, Allis R, Moore J. 2021. Geothermal battery energy storage. *Renewable Energy*. 164:777-790. Available from: <https://doi.org/10.1016/j.renene.2020.09.083>.
- Hackley PC. 2012. Geologic assessment of undiscovered conventional oil and gas resources—Middle Eocene Claiborne Group, United States Part of the Gulf of Mexico Basin. Reston (Virginia): U.S. Geological Survey. 93 p. USGS Open File Report 2012-1144. Available from: <http://pubs.usgs.gov/of/2012/1144/>.
- Hamlin HS. 2009. Ozona sandstone, Val Verde Basin, Texas: Synorogenic stratigraphy and depositional history in a Permian foredeep basin. *AAPG Bulletin*. 93(5):573-594. Available from: <https://doi.org/10.1306/01200908121>.
- Hasterok D, Webb J. 2017. On the radiogenic heat production of igneous rocks. *Geoscience Frontiers*. 8(5):919-940. Available from: <https://doi.org/10.1016/j.gsf.2017.03.006>.
- Horowitz FG, Smith JD, Wheaton CA. 2015. One dimensional conductive geothermal Python code. Available from: <https://bitbucket.org/geothermalcode/onedimensionalgeothermalheatconductionmodel.git>.
- John CJ, Maciasz G, Harder BJ. 1998a. Volume 11-A: Resource description, program history, wells tested, university and company based research, site restoration. In: John CJ, Maciasz G, Harder BJ. *Gulf Coast geopressed-geothermal program summary report compilation*. Baton Rouge (Louisiana): Basin Research Institute, Louisiana State University. 195 p. Available from: <https://doi.org/10.2172/661421>.
- John CJ, Maciasz G, Harder BJ. 1998b. Volume 11-B: Resource description, program history, wells tested, university and company based research, site restoration. In: John CJ, Maciasz G, Harder BJ. *Gulf Coast geopressed-geothermal program summary report compilation*. Baton Rouge (Louisiana): Basin Research Institute, Louisiana State University. 307 p. Available from: <https://doi.org/10.2172/661418>.
- Kincade SC. 2018. The occurrence of the Greta Sandstone, Frio Formation (Late Oligocene), Texas Gulf Coastal Plain [thesis]. Fayetteville (Arkansas): University of Arkansas. 75 p. Available from: <https://scholarworks.uark.edu/etd/2873/>.
- Kresic N. 2010. Chapter 2 - Types and classifications of springs. In: Kreis N, Stevanovic Z, editors. *Groundwater hydrology of springs*. Oxford (United Kingdom): Butterworth-Heinemann. p. 31-85. Available from: <https://www.elsevier.com/books/groundwater-hydrology-of-springs/kresic/978-1-85617-502-9?msclkid=6f35ce54c0f711ecbf-c450daff6212cd>.
- Lambert RB. 2004. Hydrogeology of Webb County, Texas. Reston (Virginia): U.S. Geological Survey. Scientific Investigations Report 2004-5022. Available from: <https://doi.org/10.3133/sir20045022>.
- Malik S. 2021 April 22. South Texas geothermal energy project ready to provide power that never stops. Reporting Texas. Available from: <https://reportingtexas.com/south-texas-geothermal-energy-project-ready-to-provide-power-that-never-stops/>.
- McDonnell A, Loucks RG, Galloway W. 2008. Paleocene to Eocene deep-water slope canyons, western Gulf of Mexico: Further insights for the provenance of deep-water offshore Wilcox Group plays. *AAPG Bulletin*. 92(9):1169-1189. Available from: <https://doi.org/10.1306/05150808014>.
- McKenna TE, Sharp JM. 1998a. Thermal Conductivity of Wilcox and Frio Sandstones in South Texas (Gulf of Mexico Basin). *AAPG Bulletin*. 80(8):1203-1215. Available from: <https://doi.org/10.1306/64ED8CE6-1724-11D7-8645000102C1865D>.
- McKenna TE, Sharp JM. 1998b. Radiogenic heat production in sedimentary rocks of the Gulf of Mexico Basin, South Texas. *AAPG Bulletin*. 82(3):484-496. Available from: <https://doi.org/10.1306/1D9BC449-172D-11D7-8645000102C1865D>.
- Moya D, Aldás C, Kaparaju P. 2018. Geothermal energy: Power plant technology and direct heat applications. *Renewable and Sustainable Energy Reviews*. 94:889-901. Available from: <https://doi.org/10.1016/j.rser.2018.06.047>.

- Negraru PT, Blackwell DD, Erkan K. 2008. Heat flow and geothermal potential in the South-Central United States. *Natural Resources Research.* 17:227-243. Available from: <https://doi.org/10.1007/s11053-008-9081-x>.
- [NGDS] National Geothermal Data System. 2014. Data exchange models. Available from: <https://www.geothermaldata.org/content-models/data-interchange-content-models>.
- [NGDS] National Geothermal Data System. 2020. SMU Node. Available from: <http://geothermal.smu.edu/>.
- NS Energy. 2020 Jan 8. Profiling the top geothermal power producing countries in the world. Available from: <https://www.nsenergybusiness.com/features/top-geothermal-power-producing-countries>.
- OpenEI.org. 2016. Texas Geothermal Permitting Process. Department of Energy Regulatory and Permitting Information Desktop Toolkit for Texas Geothermal Permitting Process. Available from: <https://openei.org/wiki/RAPID/Geothermal/Texas>.
- Pitman JK, Rowan ER. 2012. Temperature and petroleum generation history of the Wilcox Formation, Louisiana. Reston (Virginia): U.S. Geological Survey. 51 p. USGS Open File Report. 2012-1046. Available from: <https://doi.org/10.3133/ofr20121046>.
- Richards MC, Blackwell DD. 2012. Developing geothermal energy in Texas: Mapping the temperatures and resources. *Gulf Coast Association of Geological Societies Transactions.* 62:351-363. Available from: https://archives.datapages.com/data/gcags/data/062/062001/351_gcags620351.htm.
- Richards MC, Blackwell DD, Williams MA, Frone ZS, Dingwall RK, Batir JF, Chickering C. 2012. Proposed reliability code for heat flow sites. *Geothermal Resources Council Transactions.* 36:211-217. Available from: <https://www.geothermal-library.org/index.php?mode=pubs&action=view&record=1030231>.
- Richter A. 2018 Sep 12. Oil & gas firms – a strategic evaluation of an entry into the geothermal sector. Think Geo-Energy. Available from: <https://www.thinkgeoenergy.com/oil-gas-firms-a-strategic-evaluation-of-an-entry-into-the-geothermal-sector/>.
- Robertson EC. 1988. Thermal properties of rock. Reston (Virginia): U.S. Geological Survey. 110 p. Open-file Report 88-441. Available from: <https://pubs.usgs.gov/of/1988/0441/report.pdf>.
- Smith JD. 2016. Analytical and geostatistical heat flow modeling for geothermal resource reconnaissance applied in the Appalachian Basin [thesis]. Ithaca (New York): Cornell University. Available from: <https://doi.org/10.7298/X4FX77C3>.
- Smith JD, Horowitz FG. 2016. Memo 8: Thermal model methods and well database organization in GPFA-AB. In: Jordan TE, Richards MC, Horowitz FG, Camp E, Smith JD, Whealton CA, Stedinger JR, Hornbach MJ, Frone ZS, Tester JW. 2016. Low temperature geothermal play fairway analysis for the Appalachian Basin: Phase 1 Revised Report November 18, 2016. Ithaca (New York): Cornell University. p. 202-234. Available from: https://gdr.openei.org/files/899/GPFA-AB_Final_Report_with_Supporting_Documents.pdf.
- Scheyder E. 2021 July 2. GM shakes up lithium industry with California geothermal project. Reuters. Available from: <https://www.reuters.com/business/autos-transportation/gm-shakes-up-lithium-industry-with-california-geothermal-project-2021-07-02/>.
- Stutz GR, Shope EN, Aguirre GA, Batir JF, Frone ZS, Williams MA, Reber TJ, Whealton CA, Smith, JD, Richards MC, et al. 2015. Geothermal energy characterization in the Appalachian Basin of New York and Pennsylvania. *Geosphere.* 11(5):1291-1304. Available from: <https://doi.org/10.1130/GES00499.1>.
- Tester JW, Anderson B, Batchelor A, Blackwell D, DiPippo R, Drake E, Garnish J, Livesay B, Moore MC, Nichols K, et al. 2006. The future of geothermal energy: Impact of enhanced geothermal systems (EGS) on the United States in the 21st century. Cambridge (Massachusetts): Massachusetts Institute of Technology. 209 p. DOE Contract DE-AC07-05ID14517 Final Report. Available from: https://www1.eere.energy.gov/geothermal/pdfs/future_geo_energy.pdf.
- Texas Nat. Res. Code 141 § 003. Available from: <https://statutes.capitol.texas.gov/docs/NR/htm/NR.141.htm>.
- Thibedeau J. 2019 Nov 1. Innovative technology captures energy from waste heat. Power Magazine. Available from: <https://www.powermag.com/innovative-technology-captures-energy-from-waste-heat/>.
- Turchi CS, McTigue JDP, Akar S, Beckers KJ, Richards MC, Chickering C, Batir JF, Schumann HH, Tillman T, Slivensky D. 2020. Geothermal deep direct use for turbine inlet cooling in East Texas. Golden (Colorado): National Renewable Energy Lab. 62 p. NREL/TP-5500-74990. Available from: <https://doi.org/10.2172/1602704>.
- WellDatabase. 2020. The Woodlands (Texas): WellDatabase. Available from: <https://welldatabase.com/>.
- Zafar SD, Cutright BL. 2014. Texas' geothermal resource base: a raster-integration method for estimating in-place geothermal-energy resources using ArcGIS. *Geothermics.* 50:148-154. Available from: <https://doi.org/10.1016/j.geothermics.2013.09.003>.